

Effect of Turbulence Model on the Hydrodynamics of Gas–solid Fluidized Bed



Mona Mary Varghese  and Teja Reddy Vakamalla 

Abstract Fluidized bed reactors have been extensively employed in processing industries as it provides perfect mixing, efficient operation, and large heat and mass transfer rates. Understanding the particle–fluid interaction inside the bed is a significant parameter for the effective operation of the fluidized bed. This work aims to study the effect of the turbulence model on the mean solids volume fraction and mean flow field at different operating parameters (static bed height, inlet velocity). In the current numerical study, the unsteady multiphase simulations are performed in a three-dimensional fluidized bed (Gao et al. 2012) using the two-fluid model (TFM) with the kinetic theory of granular flow (KTGF) option. k - ϵ is selected to model the turbulence. Gidaspow, Syamlal and O’Brien and energy minimization multi-scale (EMMS) drag models are considered for modeling the interphase momentum exchange coefficient. The three-dimensional models could capture the flow behavior inside the turbulent fluidized bed. The numerically predicted time-averaged solid volume fraction fits well with the experimental data at the center compared to the wall using the incorporation of EMMS drag with the k - ϵ turbulence model. Similar to the experiments, a dense region is observed with descending particles near the wall and the dilute region near the center portion of the bed. It can be noted that close numerical predictions can be obtained using the selection of an appropriate drag model and turbulence model.

M. M. Varghese · T. R. Vakamalla (✉)

Department of Chemical Engineering, NIT Calicut, Calicut-Mukkam road, Kattangal, Kozhikode 673601, India

e-mail: teja@nitc.ac.in

Keywords CFD · Drag · Gas–solid fluidized bed · Hydrodynamics · Turbulence model

Nomenclature

$C_{1\epsilon}, C_{2\epsilon}, C_{3\epsilon}$ [-]	Model constant
C_d [-]	Drag coefficient
d_p [m]	Particle diameter
e [-]	Restitution coefficient
g [m s ⁻²]	Acceleration due to gravity
g_0 [-]	Radial distribution coefficient
H [m]	Axial position
H_0 [m]	Static bed height
I [-]	Stress tensor
J_{vis} [W]	Dissipation rate due to viscous damping
J_{slip} [W]	Generation rate due to viscous damping
k [J kg ⁻¹]	Turbulent kinetic energy
k_s [kg m ⁻¹ s ⁻¹]	Diffusion coefficient for granular energy
P [Pa]	Pressure
Re_p [-]	Reynolds number of particle
U_g [m s ⁻¹]	Superficial gas velocity
u [m s ⁻¹]	Velocity

Greek symbols

α [-]	Volume fraction
β [kg m ⁻³ s ⁻¹]	Interphase momentum transfer coefficient
γ [kg m ⁻¹ s ⁻³]	Collisional energy dissipation
λ [kg m ⁻¹ s ⁻¹]	Bulk viscosity
μ [kg m ⁻¹ s ⁻¹]	Shear viscosity
ρ [kg m ⁻³]	Density
τ [Pa]	Stress tensor
Θ [m ² s ⁻²]	Granular temperature

1 Introduction

Multiphase reactors are considered as the heart of many industrial processes, namely chemical, petrochemical, mineral processing, petroleum refining, and pharmaceutical industries [1]. Turbulent fluidized bed is the most prominent multiphase reactor having advantages like uniform temperature distribution, adequate particle mixing, and large surface area of contact. The benefits also include low maintenance, minimum construction cost, and the capability to fluidize a wide range of particles [2]. The continuous increase in the gas velocity causes the bubbles to disappear and the turbulent motion of the solid cluster is observed in the turbulent fluidized bed [3]. Turbulent fluidized bed reactors are one of the important units for large applications in physical and chemical processes, examples of which include the drying process, Fischer–Tropsch synthesis, production of acrylonitrile, etc.

Even though many studies are conducted in these areas, the fluidized bed reactor remains an active research area as many of the essential hydrodynamic parameters are yet to be explored. This knowledge of parameters will guide to proper design, scale-up, and will be useful for validating the numerical model predictions. The current studies on the hydrodynamic properties of turbulent fluidized beds emphasize mainly on gas–solid mixing, solid concentration, particle velocity, etc., [4]. The understanding of the hydrodynamic parameter, namely the solid concentration is critical for the scale-up, design, optimization, and modeling of industrial units. It also influences the gas–solid mixing, performance of the reactor, heat and mass transfer rate, and mainly helps to understand the interaction between two phases [5].

With the advancement of parallel computing, numerical simulation of fluidized beds has become a powerful method for analyzing the internal flow characteristics. This model helps researchers to understand the phenomena inside different types of the fluidized bed in detail as obtaining the experimental is difficult at different operating conditions [6]. The simulated results are validated with the experimental measurements of Gao et al. [7].

2 Literature Review

In the last 2 decades, CFD has become an important research tool for better understanding the fluidization process while obtaining internal fluid dynamics of the gas–solid system [8]. Mainly, TFM and Eulerian–Lagrangian approaches are used to model gas–solid flow. The Eulerian–Lagrangian approach considers the gas phase as continuous, while the particles are tracked using the Lagrangian approach and are not employed in industrial applications due to large computational costs. The TFM considers both phases as continuous and interpenetrating and is more appropriate for a fluidized bed system [9]. The coupling between phases is ensured using the momentum transfer term where the drag force is dominant. Different drag correlations are used to compute the interphase momentum exchange coefficients.

In the literature, several computational studies figured out the importance of drag force between the particle and fluid. Many researchers carried out simulation studies in bubbling fluidized beds, but only limited numerical studies are available [10, 11] in turbulent fluidized beds. Taghipour et al. [12] focused on the hydrodynamic study of a 2D gas–solid turbulent fluidized bed with spherical glass beads of diameter 250–300 μm . The adopted drag models of Syamlal and O’Brien, Gidaspow, and Wen & Yu showed a good agreement for the values of mean pressure drop, bed expansion, and qualitative gas–solid flow pattern. They suggested that further investigation of the experimental and computational study is needed for better validation. Further, Lundberg and Halvorsen [13] studied the effect of homogeneous drag models using two-dimensional grids and the experimental results were best predicted by RUC, Hill–Koch–Ladd, and Gidaspow models. Modifications based on the RUC model were performed to analyze the influence of multiple particle phases and wall functions on bubble frequencies.

As the homogeneous drag models fail to consider the effect of mesoscale structures, Li and Kwank [14] developed an EMMS model for heterogeneous flow that mainly predicts the heterogeneity inside the fluidization system. The results obtained using the EMMS model are more realistic and accurate, whereas the conventional Gidaspow and Syamlal and O’Brien drag consider a completely homogeneous condition within the computational grid. Wang et al. [15] selected the EMMS drag model to predict the hydrodynamics of a turbulent fluidized bed with FCC particles. The model suggested by Ullah et al. [16] showed close validation with experimental results using the EMMS drag model for time-averaged solid volume fraction. Shah et al. [17] compared the results obtained using EMMS and Gidaspow drag models with experimental data. Time-averaged radial and axial solid volume fraction profiles were examined using different models and found that EMMS predicted well compared to other drag models. The simulation study conducted by Shi et al. [18] and Varghese et al. [19] in a 2D and 3D turbulent fluidized showed that a combination of different numerical parameters for 2D simulation resulted in accurate predictions. Whereas, it is noted that the simulations conducted using the 3D model were less sensitive to the variation in numerical parameters. Further, it is observed that the 3D simulations are rather very few in the literature as a result of high computational costs. Thus, the hydrodynamics in the turbulent gas–solid fluidized bed was investigated computationally in this work using the 3D model.

3 Scope of Work

From the previous works, it is noted that a large number of the studies consider the system as homogeneous, neglecting the influence of heterogeneous flow structures mainly in the turbulent fluidized bed. Firstly, this study is based on the experimental work of Gao et al. [7] and mainly focuses on understanding the solid flow properties inside the gas–solid turbulent fluidized bed for different operating conditions. It also aims to understand the importance of drag models on the turbulent fluidization

regime by assessing the flow predictions, i.e., solids volume fraction. The drag models considered for this study include the Gidaspow, Syamlal and O'Brien, and EMMS models. The above drag models are tested to find their capability in predicting accurate flow dynamics in turbulent fluidization conditions. This work mainly focuses on understanding the importance of selecting an appropriate drag model and turbulence model on the numerical prediction of hydrodynamic behavior in a turbulent fluidized bed. Further, the CFD predicted flow properties (solids volume fraction and particle velocity) are validated against the experimental measurements of Gao et al. [7].

4 Model Description

4.1 Governing Equation

Here, both the phases are modeled using the Eulerian-Eulerian two-fluid approach. Both the phases are assumed to be an interpenetrating continuum. The phase changes and chemical reactions are not considered in this study. The hydrodynamic model used for gas–solid fluidization primarily uses the principles of conservation of mass and momentum. Different ways are used to formulate the two-fluid flow model depending on the averaging procedure and closure law. Here, the integral balance of mass and momentum for a fixed control volume is adopted for both continuous and discrete phases. Anderson & Jackson [20] and Ishii [21] derived governing equations for two-fluid flow.

The mass conservation equation for gas and solid phase:

$$\frac{\partial(\alpha_g \rho_g)}{\partial t} + \nabla \cdot (\alpha_g \rho_g u_g) = 0 \quad (1)$$

$$\frac{\partial(\alpha_s \rho_s)}{\partial t} + \nabla \cdot (\alpha_s \rho_s u_s) = 0 \quad (2)$$

Here, $\alpha_g + \alpha_s = 1$.

where subscript g-gas phase and s-solid phase.

This equation is used for calculating the volume fraction for each phase. The momentum equation:

For gas phase,

$$\frac{\partial(\alpha_g \rho_g u_g)}{\partial t} + \nabla \cdot (\alpha_g \rho_g u_g u_g) = -\alpha_g \nabla P + \nabla \cdot (\alpha_g \tau_g) + \beta(u_s - u_g) + \alpha_g \rho_g g \quad (3)$$

For solid phase,

$$\frac{\partial(\alpha_s \rho_s u_s)}{\partial t} + \nabla \cdot (\alpha_s \rho_s u_s u_s) = -\alpha_s \nabla P - \nabla P_s + \nabla \cdot (\alpha_s \tau_s) + \beta(u_g - u_s) + \alpha_s \rho_s g \quad (4)$$

Further, the constitutive relations for the solid phase stress are derived by Lun et al. [22]. The equation used is as follows:

$$P_s = \alpha_s \rho_s \Theta + 2\alpha_s^2 \rho_s g_0 \Theta (1 + e) \quad (5)$$

The radial distribution function is given by the equation

$$g_0 = \left[1 - \left(\frac{\alpha_s}{\alpha_{s,\max}} \right)^{1/3} \right]^{-1} \quad (6)$$

$\alpha_{s,\max}$ - maximum volume fraction of particles.

The solid bulk viscosity that considers the resistance of granular particles is calculated by Lun et al. [23] from the equation

$$\lambda_s = \frac{4}{3} \alpha_s^2 \rho_s d_p g_0 (1 + e) \sqrt{\frac{\Theta}{\Pi}} \quad (7)$$

The transport equation of granular temperature is given by the equation

$$\begin{aligned} \frac{3}{2} \left[\frac{\partial(\alpha_s \rho_s \Theta)}{\partial t} + \nabla \cdot (\alpha_s \rho_s u_s \Theta) \right] &= (-P_s I + \tau_s) : \nabla u_s \\ + \nabla \cdot (k_s \nabla \Theta) - \gamma_s + J_{vis} + J_{slip} & \quad (8) \end{aligned}$$

where the first term on the right-hand side corresponds to the generation of granular energy; the diffusion of granular temperature is denoted by the second term; the dissipation of granular energy is represented by the third term; the last term corresponds to the energy exchange between the phases.

Turbulence model:

The standard k- ϵ model is given by the equation

$$\begin{aligned} \frac{\partial(\rho k)}{\partial t} + \frac{\partial(\rho k u_i)}{\partial x_i} &= \frac{\partial}{\partial x_j} \left[\left(\mu + \frac{\mu_t}{\sigma_k} \right) \frac{\partial k}{\partial x_j} \right] + G_k + G_b - \rho \epsilon - Y_M + S_k \\ \frac{\partial(\rho \epsilon)}{\partial t} + \frac{\partial(\rho \epsilon u_i)}{\partial x_i} &= \frac{\partial}{\partial x_j} \left[\left(\mu + \frac{\mu_t}{\sigma_k} \right) \frac{\partial \epsilon}{\partial x_j} \right] + C_{1\epsilon} \frac{\epsilon}{k} (C_{1k} + C_{3\epsilon} G_b) - C_{2\epsilon} \rho \frac{\epsilon^2}{k} + S_\epsilon \end{aligned}$$

4.2 Interphase Momentum Exchange

The drag force correlations used in the simulations are as follows:

1. Gidaspow Drag Model [24]:

It is a homogeneous drag model obtained by combining the Wen and Yu [25] and Ergun [26] equations. The equation used to evaluate the interphase momentum transfer coefficient is

$$\beta = \frac{150 \alpha_s^2 \mu_g}{\alpha_g d_p^2} + \frac{1.75 \alpha_s \rho_g |u_g - u_s|}{d_p} \text{ for } \alpha_g \leq 0.8$$

$$\beta = \frac{3 \alpha_s \alpha_g}{4 d_p} \rho_g |u_g - u_s| C_{d,isol} \alpha_g^{-2.65} \text{ for } \alpha_g > 0.8$$

Where

$$C_{d,isol} = \begin{cases} 0.44 & \text{for } \text{Re}_p \geq 1000 \\ 24/\text{Re}_p (1 + 0.15 \text{Re}_p^{0.687}) & \text{for } \text{Re}_p < 1000 \end{cases} \quad (9)$$

2. Syamlal and O'Brien Drag Model [27]:

This equation is based on the terminal velocity of a single particle in a fluid.

$$\beta = \frac{3 \alpha_s \alpha_g}{4 u_{rs}^2 d_p} \rho_g C_{d,isol} |u_g - u_s|$$

Where

$$C_{d,isol} = \left(0.63 + \frac{4.8}{\sqrt{\text{Re}_p / u_{rs}}} \right)^2$$

$$u_{rs} = 0.5 \left(A - 0.06 \text{Re}_p + \sqrt{(0.06 \text{Re}_p)^2 + 0.12 \text{Re}_p (2B - A) + A^2} \right)$$

$$A = \alpha_g^{4.14}$$

$$B = \begin{cases} 0.8 \alpha_g^{1.28} & \text{for } \alpha_g \leq 0.85 \\ \alpha_g^{2.65} & \text{for } \alpha_g > 0.85 \end{cases} \quad (10)$$

3. Energy Minimization Multiscale (EMMS) Drag Model [14, 28]:

It is based on energy minimization for the transport and suspension of particles.

$$\beta = \frac{150 (\alpha_s)^2 \mu_g}{(1 - \alpha_s) d_p^2} + \frac{1.75 \alpha_s \rho_g |u_g - u_s|}{d_p} \text{ for } \alpha_s \geq 0.26$$

$$\beta = \frac{3}{4} \frac{\alpha_s (1 - \alpha_s)}{d_p} \rho_g |u_g - u_s| C_{d,isol} \omega(\alpha_s) \text{ for } \alpha_s < 0.26$$

Where

$$\omega(\alpha_s) = -0.5760 + \frac{0.0214}{4((1 - \alpha_s) - 0.7463)^2 + 0.0044} \text{ for } 0.18 \leq \alpha_s < 0.26$$

$$\omega(\alpha_s) = -0.0101 + \frac{0.0038}{4((1 - \alpha_s) - 0.7789)^2 + 0.0040} \text{ for } 0.03 \leq \alpha_s < 0.18$$

$$\omega(\alpha_s) = -31.8295 + 32.8295(1 - \alpha_s) \text{ for } \alpha_s < 0.03 \quad (11)$$

4.3 Numerics

The experimental measurements of Gao et al. [7] are used to validate the present 3D simulation study conducted in a cylindrical turbulent fluidized bed with dimensions as shown in Fig. 1a. The glass beads with a mean diameter of 130 μm and a density of 2400 kg/m^3 are used in this study. The experiments are conducted using the multifunctional optical fiber probe in the Gao et al. [7] study.

The granular option enabled TFM model coupled with the laminar, and the k- ϵ turbulence model is used for the simulation study in turbulent fluidized beds. The interphase drag force models of Gidaspow [24], EMMS [14], and Syamlal and O'Brien [27] are considered to model the interphase momentum transfer coefficient. The new drag models are introduced using user defined functions (UDFs) in ANSYS Fluent 20.1. The particle properties are described using the KTGF.

The fine mesh is created near the wall to accurately predict the velocity distribution near-wall region. The grid independence test is performed with three different meshes of size varying from 42,680 to 1,07,520 nodes. The corresponding grid independence test data using the EMMS drag model are shown in Fig. 1b.

The boundary conditions of the velocity inlet and the pressure outlet are specified at the column inlet and the outlet. For the gas phase, a no-slip condition is used at the walls. The partial slip for the solid phase with a specular coefficient of 0.6 is used based on Passalacqua and Marmo [29] for the turbulent fluidized bed. The particle restitution coefficient that represents the granular phase collisions is given a value of 0.95 [30]. The convective terms of the transport equations are solved using the quadratic upstream interpolation for convective kinematics (QUICK) scheme. A second-order implicit scheme is selected for the time discretization. The semi-implicit method for pressure linked equations (SIMPLE) algorithm is considered for the pressure and velocity coupling. For the turbulence calculation, the laminar and k- ϵ models are used. A maximum of 20 iterations per time step is applied, and

Table 1 Summary of variables used in simulation studies

Variables	Values
Inlet gas velocity, ms^{-1}	0.94, 1.10, 1.25
Particle diameter, μm	139
Static bed height, m	0.096, 0.151, 0.204
The angle of internal friction, $^{\circ}$	28
Time step, s	10^{-4}
Simulation time, s	30
Iterations per time step	20
Restitution coefficient	0.95
Specularity coefficient	0.6
Coefficient of lift	0.25
Turbulence model	Laminar and K- ϵ
Drag model	Gidaspow, Syamlal and O'brien, EMMS

the residual is specified to be 0.0001 for the convergence criteria. The summary of variables used for the numerical simulations is provided in Table 1.

5 Results and Discussion

5.1 Grid Independence Test

Figure 1b represents the time-averaged void fraction for different grid sizes. It is calculated for a superficial velocity of 1.25 m/s and a static bed height of 0.151 m. The results are plotted at an axial position of 0.338 m. It is observed that both the 70 k and 100 k mesh are giving close predictions with the experimental results. While the coarser-sized mesh (~ 42 k) could not capture the correct behavior of particles inside the bed. So it is concluded that the medium size mesh (~ 70 k) can be selected for further study. Also, due to the large computational time, the use of finer mesh is not recommended.

5.2 Effect of Drag Models

Initially, a 3D cylindrical column with a uniform inlet superficial velocity of 1.25 m/s is considered for running the numerical simulation. The gas is injected uniformly through the bottom of the bed. A static bed height of 0.151 m is maintained before

initializing the simulation. As time passes, it is noted that the bed gets expanded, which leads to the complete mixing of solid particles.

The time-averaged experimental void fraction data show a symmetric behavior in the radial direction. When Gidaspow, Syamlal and O'Brien, and EMMS models are compared, it is observed that the EMMS drag model gives close predictions. The conventional drag model is largely deviated and fails to include the effect of clusters. The presence of particle clusters is mainly observed near the wall because of the low particle velocity at the wall. Also, it is noted that the solid distribution is dilute in the middle compared to the dense portion near the wall. A large deviation is noticed with the Gidaspow drag model as it causes higher bed expansion and neglects the presence of mesoscale structures. At a higher inlet velocity, more phase interactions and larger turbulence (Fig. 2) are present. This can be clearly analyzed by using the structure-dependent EMMS drag model.

5.3 *Effect of Turbulence Models*

Fluctuating and chaotic behavior are the main characteristics of turbulent flow. The effect of turbulence increases with an increase in velocity. It is clear from Fig. 3 that both the particle clusters and bubbles are present inside the turbulent fluidized bed. Simulations are performed with the selected EMMS drag model using the laminar and k- ϵ turbulence models. In the laminar flow, no turbulence parameter is present in the set of equations while the k- ϵ model is an empirical model based on the model transport equations for the turbulence kinetic energy and the dissipation rate. The standard k- ϵ model used to model the turbulence in the gas phase shows superior results. It is also noted that the k- ϵ model reveals better predictions of solid volume fraction both in the core and near the wall region. Moreover, the k- ϵ model is used for a wide range of applications in turbulent flows due to its easy convergence and low memory requirement. It is also noted that the laminar model is giving better predictions at the top dilute region of the bed.

5.4 *Comparison of Simulated and Experimental Results*

Radial time-averaged solid volume fraction. The results obtained for time-averaged solid volume fraction using the EMMS drag model and k- ϵ turbulence model in the radial direction are compared against the experimental data and shown in Fig. 4. It is noted that better predictions are observed near the center of the column. The increase in velocity of gas causes the bubbles to rise and coalesce, forming larger bubbles. It finally breaks at the free surface. The solid distribution with the dilute center and a dense region near the wall can be observed from Fig. 3. It is noted that the simulation results agree well at the bottom dense region, while the upper dilute zone results are underestimated. The EMMS model shows close predictions with

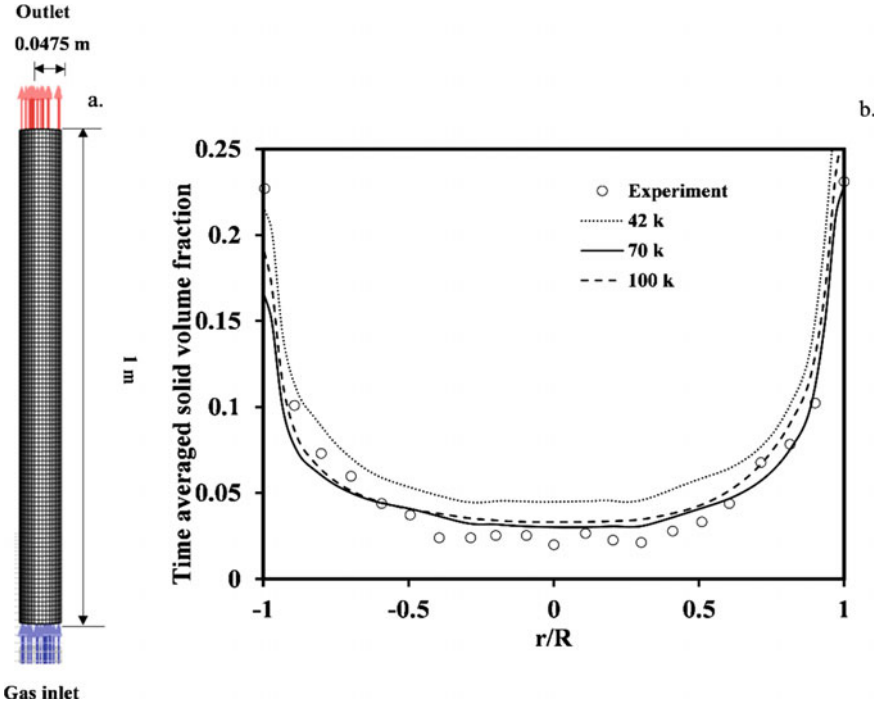


Fig. 1 a 3D mesh used for turbulent fluidized bed simulations, b mesh independence study in the turbulent fluidized bed for a velocity of 1.25 m/s and a static bed height of 0.151 m [7]

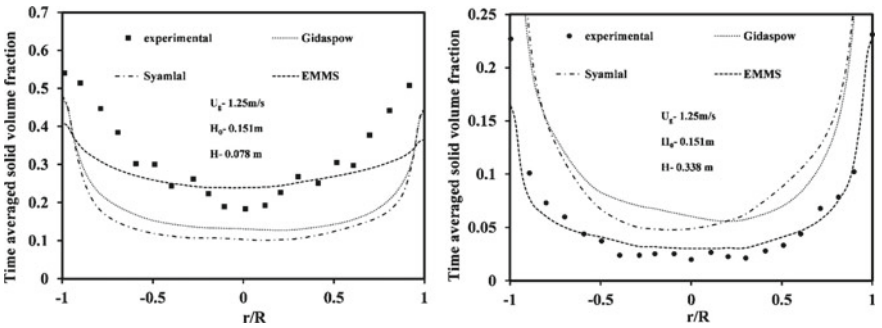


Fig. 2 CFD predicted radial variation of time-averaged solid volume fraction compared against experimental data [7] using different drag models at two different axial heights with 1.25 m/s of inlet gas velocity

Fig. 3 CFD predicted instantaneous solid volume fraction contours of the 3D fluidized bed using the EMMS drag model with $k-\epsilon$ turbulence model for the superficial gas velocity of 1.25 m/s

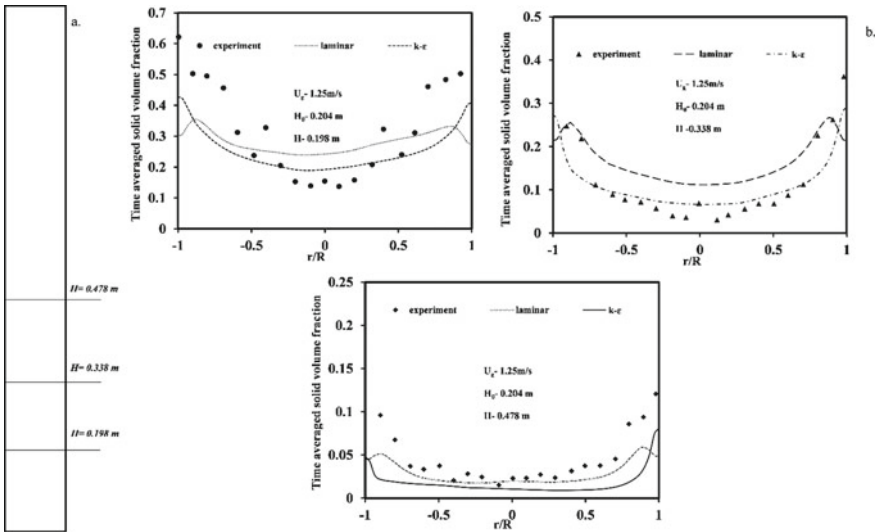
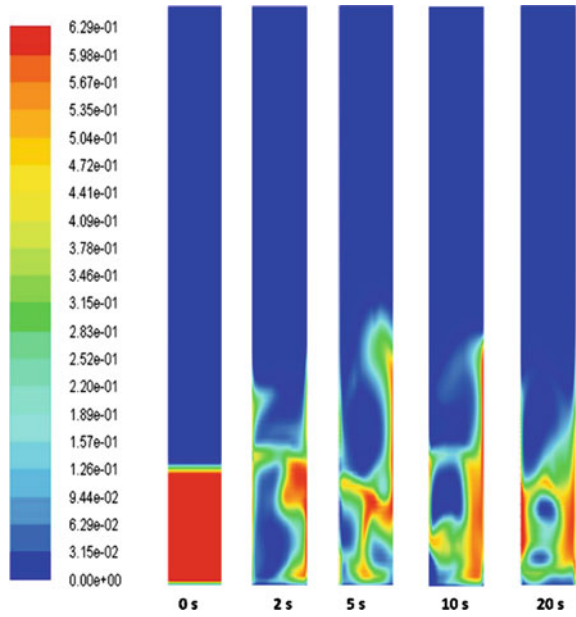


Fig. 4 a Outline of fluidized bed indicating different axial positions, b CFD predicted time-averaged solid volume fraction compared against experimental data [7] along the radial direction using two turbulence models at different axial heights for the inlet gas velocity of 1.25 m/s

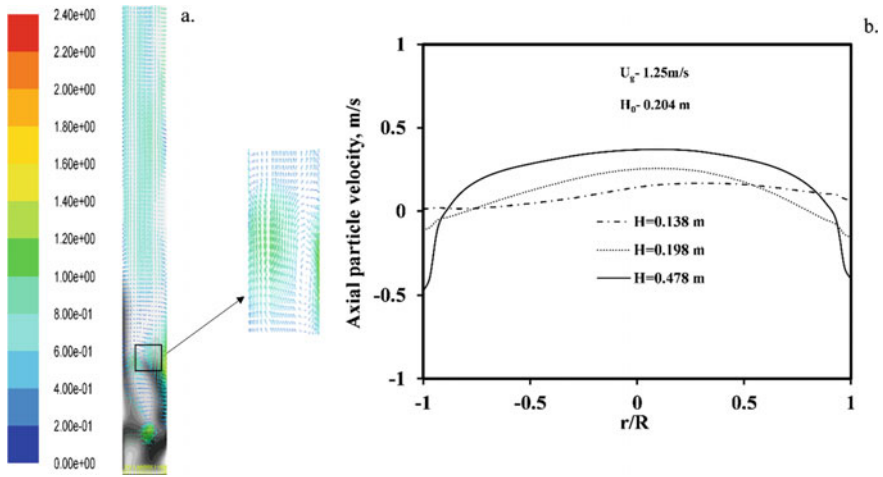


Fig. 5 **a** Void fraction contour and solid velocity vector in a 3D turbulent fluidized bed for the superficial velocity of 1.25 m/s, **b** Radial distribution of the axial solid velocities at different axial positions

the experimental results as it considers the effect of the mesoscale structure formed inside the bed.

It is found that the predicted solid volume fraction data are lower near the wall, whereas it is higher near the center compared to the experimental measurements. This may be due to the assumptions of the mean particle diameter instead of particle size distribution [7].

Particle velocity profile. The properties displayed by a fluidized bed mainly depend upon the velocity of particles, i.e., the movement of particles inside the bed. The solid particles always tend to move away from the center of the bed. This is because the gas in the form of bubbles tends to move upward and coalesces to form a larger bubble. Figure 5a shows the void fraction contour and solid velocity vector for a superficial velocity of 1.25 m/s using the EMMS drag model. In all the cases, high voidage is observed at the center and the particle-rich phase is found adjacent to the wall. In general, the velocity is positive near the center and approaches negative toward the wall. The negative velocities near the wall are expected due to the particle’s back mixing. It is noticed from Fig. 5b that the radial profile of axial velocity increases with the axial position. The rise in particle velocity also improves the mixing of particles inside the bed.

6 Conclusions

- The characteristics of the gas–solid flow behavior in the turbulent fluidized bed are investigated using CFD simulations.

- The TFM with structure-dependent EMMS drag model and k- ϵ turbulence model able to predict the close void fraction data compared to experiments.
- From the transient local solid fraction contour, it is clear that the dilute phase exists near the center while the dense phase exists near the wall.
- The presence of the dilute top region of the bed causes the discrepancy in height in the case of radial solid fraction.
- The simulated time-averaged radial solid fraction shows close approximations with the experimental data, and the solid velocities at different axial positions are numerically analyzed.

References

1. Rüdüsüli, M., Schildhauer, T.J., Biollaz, S.M., van Ommen, J.R.J.P.T.: Scale-up of bubbling fluidized bed reactors—A review. *Powder Technology* 217, 21–38 (2012)
2. Daizo, K., Levenspiel, O.: *Fluidization engineering*, 2nd edn. Butterworth Publishers, United States (1991)
3. Drake, J.: *Hydrodynamic characterization of 3D fluidized beds using noninvasive techniques*. Graduate Theses and Dissertations. Iowa State University (2011)
4. Ellis, N., Bi, H.T., Lim, J., Grace, J.: Hydrodynamics of Turbulent Fluidized Beds of Different Diameters. *Powder Technol.* **141**, 124–136 (2004)
5. Mostoufi, N., Chaouki, J.: Local Solid Mixing in Gas-Solid Fluidized Beds. *Powder Technol.* **114**, 23–31 (2001)
6. Zhou, L., Zhang, L., Bai, L., Shi, W., Li, W., Wang, C., Agarwal, R.: Experimental study and transient CFD/DEM simulation in a fluidized bed based on different drag models. *RSC Adv.* **7**(21), 12764–12774 (2017)
7. Gao, X., Wu, C., Cheng, Y.-W., Wang, L.-J., Li, X.: Experimental and numerical investigation of solid behavior in a gas–solid turbulent fluidized bed. *Powder Technol.* **228**, 1–13 (2012)
8. Sau, D.C., Biswal, K.C.: Computational fluid dynamics and experimental study of the hydrodynamics of a gas–solid tapered fluidized bed. *Appl. Math. Model.* **35**(5), 2265–2278 (2011)
9. Hamzehei, M.: CFD modeling and simulation of hydrodynamics in a fluidized bed dryer with experimental validation. *International Scholarly Research Notices* 2011, (2011)
10. Chang, J., Wu, Z., Wang, X., Liu, W.: Two- and three-dimensional hydrodynamic modeling of a pseudo-2D turbulent fluidized bed with Geldart B particle. *Powder Technol.* **351**, 159–168 (2019)
11. Wu, Y., Shi, X., Gao, J., Lan, X.: A four-zone drag model based on cluster for simulating gas-solids flow in turbulent fluidized beds. *Chemical Engineering and Processing—Process Intensification* 155, 108056 (2020)
12. Taghipour, F., Ellis, N., Wong, C.: Experimental and computational study of gas–solid fluidized bed hydrodynamics. *Chem. Eng. Sci.* **60**(24), 6857–6867 (2005)
13. Lundberg, J., Halvorsen, B.M.: A review of some existing drag models describing the interaction between phases in a bubbling fluidized bed. *Proc 49th Scandinavian Conference on Simulation and Modeling (SIMS 2008)*, pp. 7–8. Oslo, Norway (2008)
14. Li, J., Kwauk, M.: *Particle-Fluid Two-Phase Flow: the Energy-Minimization Multi-Scale Method*. Metallurgical Industrial Press, Beijing (1994)
15. Wang, B., Li, T., Sun, Q.-W., Ying, W.-Y., Fang, D.-Y.: Experimental Investigation on Solid Concentration in Gas-Solid Circulating Fluidized Bed for Methanol-to-Olefins Process. *Int. J. Chem. Eng.* **4**(8), 494–500 (2010)

16. Ullah, A., Jamil, I., Hamid, A., Hong, K.: EMMS mixture model with size distribution for two-fluid simulation of riser flows. *Particuology* **38**, 165–173 (2018)
17. Shah, M.T., Utikar, R.P., Tade, M.O., Pareek, V.K.J.C.E.J.: Hydrodynamics of an FCC riser using energy minimization multiscale drag model. *Chem. Eng. J.* **168** (2), 812–821 (2011)
18. Shi, H., Komrakova, A., Nikrityuk, P.J.P.T.: Fluidized beds modeling: Validation of 2D and 3D simulations against experiments. *Powder Technol.* **343**, 479–494 (2019)
19. Varghese, M.M., Vakamalla, T.R., Mantravadi, B., Mangadoddy, N.: Effect of Drag Models on the Numerical Simulations of Bubbling and Turbulent Fluidized Beds. *Chem. Eng. Technol.* **44**(5), 865–874 (2021)
20. Anderson, T.B., Jackson, R.: Fluid Mechanical Description of Fluidized Beds. *Equations of Motion. Industrial & Engineering Chemistry Fundamentals* **6** (4), 527–539 (1967).
21. Ishii, M.: *Thermo-fluid dynamic theory of two-phase flow*. Eyrolles, [Paris] (1975).
22. Van der Hoef, M.A., Ye, M., Van Sint Annaland, M., Andrews, A.T., Sundaresan, S., Kuipers, J.A.M.: *Multiscale Modeling of Gas-Fluidized Beds*. Academic Press (2006)
23. Lun, C.K.K., Savage, S.B., Jeffrey, D.J., Chepurmy, N.: Kinetic theories for granular flow: inelastic particles in Couette flow and slightly inelastic particles in a general flowfield. *J. Fluid Mech.* **140**, 223–256 (1984)
24. Gidaspow, D.: *Multiphase flow and fluidization: continuum and kinetic theory descriptions*. Academic press (1994)
25. Wen, C.Y.: *Mechanics of fluidization*. Chemical engineering progress symposium series, pp. 100–111. (1966)
26. Ergun, S.: Fluid flow through packed columns. *Chem. Eng. Prog.* **48**, 89–94 (1952)
27. Syamlal, M., O'Brien, T.: The derivation of a drag coefficient formula from velocity-voidage correlations. Technical Note, US Department of energy, Office of Fossil Energy, West Virginia, (1987)
28. Yang, N., Wang, W., Ge, W., Wang, L., Li, J.: Simulation of heterogeneous structure in a circulating fluidized-bed riser by combining the two-fluid model with the EMMS approach. *Industrial Engineering Chemistry Research* **43** (18), 5548–5561 (2004)
29. Passalacqua, A., Marmo, L.J.C.E.S.: A critical comparison of frictional stress models applied to the simulation of bubbling fluidized beds. *Chemical Engineering Science* **64** (12), 2795–2806 (2009)
30. Loha, C., Chattopadhyay, H., Chatterjee, P.K.: Effect of coefficient of restitution in Euler-Euler CFD simulation of fluidized-bed hydrodynamics. *Particuology* **15**, 170–177 (2014)